

Theoretical study on intervalence band absorption in InPbased quantum well laser structures

Taehee Cho, Hyungsuk Kim, Youngse Kwon, and Songcheol Hong

Citation: *Appl. Phys. Lett.* **68**, 2183 (1996); doi: 10.1063/1.116006

View online: <http://dx.doi.org/10.1063/1.116006>

View Table of Contents: <http://apl.aip.org/resource/1/APPLAB/v68/i16>

Published by the [American Institute of Physics](#).

Additional information on *Appl. Phys. Lett.*

Journal Homepage: <http://apl.aip.org/>

Journal Information: http://apl.aip.org/about/about_the_journal

Top downloads: http://apl.aip.org/features/most_downloaded

Information for Authors: <http://apl.aip.org/authors>

ADVERTISEMENT



Goodfellow
metals • ceramics • polymers • composites
70,000 products
450 different materials
small quantities fast

www.goodfellowusa.com

Theoretical study on intervalence band absorption in InP-based quantum-well laser structures

Taehee Cho,^{a)} Hyungsuk Kim, Youngse Kwon, and Songcheol Hong

Opto-Electronics Research Center, Department of Electrical Engineering, Korea Advanced Institute of Science and Technology, Kusong-Dong, Yousong-Gu, Taejeon 305-701, Korea

(Received 27 November 1995; accepted for publication 13 February 1996)

Intervalence band absorptions of 1.5 μm light in various InGaAs/InGaAsP quantum well laser structures are investigated theoretically. The intervalence band absorption formalism based on 6×6 Luttinger-Kohn Hamiltonian is developed. The absorption tends to decrease with the barrier height of quantum wells. The tensile strain in the well causes the absorption to reduce, while the compressive strain causes it to increase. Also is found that the absorption decreases with increase in temperature. © 1996 American Institute of Physics. [S0003-6951(96)04416-8]

Quantum well (QW) lasers are widely used due to their low threshold currents and their temperature insensitive behavior.¹ The efficiency of InP-based long wavelength QW lasers depends on the optical losses in the structures and therefore it is important to understand the optical loss mechanisms. The well known optical loss mechanisms in these QWs are the Auger recombination,^{2,3} intervalence band absorption (IVBA),⁴⁻⁷ and carrier leakage over heterobarriers.^{8,9} Though, a theoretical work on the less temperature dependence of Auger recombination rates in strained-layer QW lasers is reported,¹⁰ no theoretical investigation on the optical loss due to IVBA in these structures have been reported yet.

In this letter, we report the effects of the barrier material and strain in the QW on the optical losses in InP-based QW laser structures. We have investigated the IVBA of the conventional QW laser structures such as InGaAs/InGaAsP (1.3 μm), InGaAs/InGaAsP (1.15 μm) and InGaAs/InP QWs. Since the threshold currents of such QW lasers are reduced by the biaxial compressive and tensile strains in the well, these effects have also been included in our investigation.

Since the spin orbit coupling in InP-based structures is strong, the 6×6 Luttinger-Kohn Hamiltonian is used to calculate the valence band structures of QWs.¹¹ The strain matrix was added to consider the effect of strain on the optical losses in QW structures.¹¹ The extended states were calculated by assuming that $\phi(0) = \phi(L) = 0$, where L is the boundary of the barrier for the QW structures. In our calculations we have assumed large L so as to avoid the quantization effects of eigenstates above the barrier. In the present study we assumed $L = 600 \text{ \AA}$. The valence-band offset for lattice-matched InGaAs/In_{1-x}Ga_xAs_yP_{1-y} was calculated using the relation¹²

$$\Delta E_v = 350 - 502y + 152y^2 \text{ meV.} \quad (1)$$

The other parameters such as lattice constants, Poisson ratios, deformation potential, spin-orbit split-off energy and Luttinger parameters used in our calculations are linearly interpolated from the bulk constants of GaAs and InAs.¹³

The absorption coefficient of the QW structures can be written as¹⁴

$$\alpha_{nn'}(\omega) = \frac{4\pi^2 e^2}{\epsilon m_0^2 \omega c} \times \sum_{k_{\parallel}} [f_n(k_{\parallel}) - f_{n'}(k_{\parallel})] |\hat{\epsilon} \cdot \mathbf{P}_{nn'}(k_{\parallel})|^2 \times \frac{1}{\pi} \frac{\hbar/\tau}{[|E_{n'}(k_{\parallel}) - E_n(k_{\parallel})| - \hbar\omega]^2 + [\hbar/\tau]^2}. \quad (2)$$

The momentum matrix is derived and described as

$$\hat{\epsilon} \cdot \mathbf{P}_{nn'} = \hbar \hat{\epsilon} \cdot \sum_{\nu, \nu'} (P_{\nu\nu'} O_{\nu\nu'}^{nn'} + Q_{\nu\nu'} D_{\nu\nu'}^{nn'}), \quad (3)$$

where P and Q are momentum matrices which depend on x-y and z momentum components, respectively and can be expressed as

$$\begin{pmatrix} A_1 & B & C & 0 & D & E \\ B^* & A_2 & 0 & C & F & G \\ C^* & 0 & A_2 & -B & G & F \\ 0 & C^* & -B^* & A_1 & -E^* & D \\ D^* & F^* & G^* & -E & H & 0 \\ E^* & G^* & F^* & D^* & 0 & H \end{pmatrix}, \quad (4)$$

where the matrix elements, A_1 , A_2 , B , C , D , E , F , G , and H are summarized in Table I.

To investigate the effect of barrier material on the optical loss, we considered three typical structures of lattice-matched InGaAs/InGaAsP single QWs. These structures, InGaAs/InP, InGaAs/InGaAsP (1.15 μm), and InGaAs/InGaAsP (1.3 μm) are hereafter referred as structure A, B, and C, respectively. The well layer considered for all these

TABLE I. Coefficients of in-plane elements defining the matrices $\hat{\epsilon} \cdot P$ and $\hat{\epsilon} \cdot Q$.

	$\hat{\epsilon}_{\parallel} \cdot P$	$\hat{\epsilon}_{\parallel} \cdot Q$
A_1	$-(\gamma_1 + \gamma_2)k_x$	0
A_2	$-(\gamma_1 - \gamma_2)k_x$	0
B	0	$i2\sqrt{3}\gamma_3$
C	$-\sqrt{3}\gamma_2k_x + i2\sqrt{3}\gamma_3k_z$	0
D	0	$-\sqrt{6}\gamma_3$
E	$i\sqrt{6}\gamma_2k_x + 2\sqrt{6}\gamma_3k_y$	0
F	$i\sqrt{2}\gamma_2k_x$	0
G	0	$-3\sqrt{2}\gamma_3$
H	$-\gamma_1k_x$	0

^{a)}Electronic mail: thcho@eekaist.kaist.ac.kr

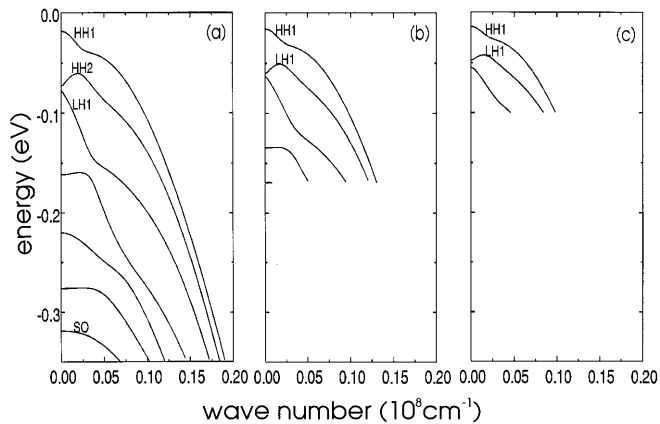


FIG. 1. The valence-band structures of (a) InGaAs/InP, (b) InGaAs/InGaAsP ($\lambda_g = 1.15 \mu\text{m}$), and (c) InGaAs/InGaAsP ($\lambda_g = 1.3 \mu\text{m}$). All the structures are lattice-matched to InP and have the well-widths of 70 \AA . The zero energy is chosen to be the top of the bulk valence-band.

structures was $\text{In}_{0.53}\text{Ga}_{0.47}\text{As}$ with a well width of 70 \AA . Figure 1 illustrates the calculated in-plane band structures of the structure A, B, and C. It can be observed from Fig. 1. that the band offset for structure A is so large that SO bands appear under the barrier potential. In the case of structures B and C, the LH1 band is followed by HH2 band and no SO band appear under the barrier potential because of the small band offset.

The temperature dependence of absorption coefficient for these lattice matched QWs, in the range (240-340 K) at the wavelength of $1.55 \mu\text{m}$, calculated using Eq. (2) is shown in Fig. 2. The temperature dependence is incorporated in the absorption coefficient by varying the Fermi-Dirac distribution. The in-plane mass of HH1 band calculated from the bandstructure, is the heaviest in the structure C and the lightest in the structure A. Therefore, the density of states of HH1 band is the smallest in the structure A. This leads to the largest overlap between Fermi-Dirac function and HH1 band for the structure A, at the same hole density of $2 \times 10^{18} \text{ cm}^{-3}$. Thus, the $\text{HH1} \rightarrow \text{extended states}$ absorption is larger in the structure A than in the structure B. However, the $\text{HH1} \rightarrow \text{extended states}$ absorption is larger in the structure C than in the structure A because of the stronger oscillator strength for transition from HH1 state to *extended states* in the struc-

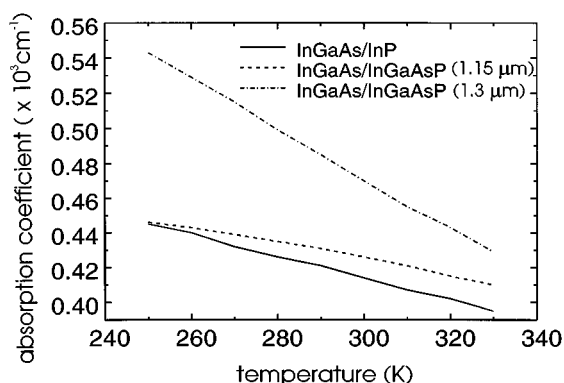


FIG. 2. IVBA coefficients with respect to temperature for the lattice-matched $\text{In}_{0.53}\text{Ga}_{0.47}\text{As}/\text{In}_{1-x}\text{Ga}_x\text{As}_y\text{P}_{1-y}$ QWs.

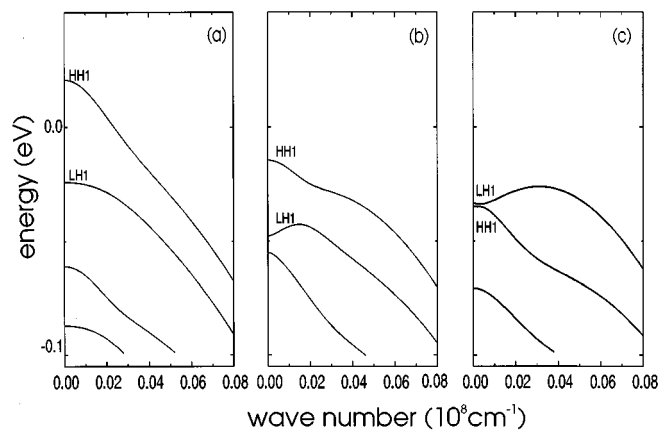


FIG. 3. The valence-band structures of three strained $\text{In}_{1-x}\text{Ga}_x\text{As}/\text{InGaAsP}$ ($\lambda_g = 1.3 \mu\text{m}$) QWs with (a) $x=0.68$, (b) $x=0.47$, and (c) $x=0.55$. All the structures have the well-widths of 70 \AA .

ture C. For the excited states, the separation between the states and Fermi level is the key factor for absorption. The absorption from LH1 or HH2 state to *extended states* can not be ignored because of the very long tail of Fermi-Dirac function at room temperature. The separation between the first excited state and Fermi level is the smallest in the structure C, thereby leading to the largest absorption coefficient from the first excited state in the structure C. Therefore, the total IVBA at $1.55 \mu\text{m}$ wavelength is the largest in the structure C (which has weak confinement potential) and the smallest in the structure A (which has strong confinement potential).

Three strained InGaAs/InGaAsP ($1.3 \mu\text{m}$) QWs were considered to examine the effects of strain on IVBA. These structures, hereafter referred as structure D, E, and F, have wells of $\text{In}_{1-x}\text{Ga}_x\text{As}$ with $x=0.32$, 0.47 , and 0.55 , respectively. The structure E is lattice-matched and therefore can be compared with structure C. The well of structure D has biaxial compressive strain, while the structure F has biaxial tensile strain, respectively. The bandstructures calculated for the structure D, E, and F are shown in Fig. 3. It can be observed from Fig. 3 that the LH1 band for the structure F is slightly above HH1 band at $k_{\parallel}=0$, due to the tensile strain in the well. It is well understood that the compressive strain drastically reduces the density of states of the HH1 band, while the tensile strain increases the density of states at the band edge. Therefore, it can be inferred that the Fermi level is located inside the HH1 band for the structure D and far from the LH1 band for the structure F.

The temperature dependence of absorption coefficients of the strained QWs in the range of 240-340 K, at the wavelength of $1.55 \mu\text{m}$ is shown in Fig. 4. The contribution of holes to IVBA is more in the structure D than in any other structure because Fermi level of the structure D is located inside the HH1 band at room temperature. As a result, the IVBA is the largest in the structure D and the smallest in the structure F.

We have observed that the absorption coefficient shows a negative temperature dependence for all the structures (A, B, C, D, E, and F). This behavior can be attributed to the decrease in the hole contribution to IVBA with increase in temperature and the upward movement of Fermi level with

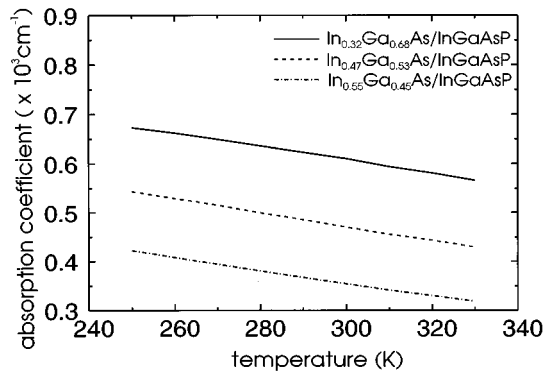


FIG. 4. IVBA coefficients with respect to temperature for the strained $\text{In}_{1-x}\text{Ga}_x\text{As}/\text{InGaAsP}$ ($\lambda_g = 1.3 \mu\text{m}$) QWs.

increase in temperature. These results are consistent with the results of Seki *et al.*¹⁰ and Asada *et al.*⁶

In conclusion we calculated the IVBA coefficients for lattice-matched and strained $\text{InGaAs}/\text{InGaAsP}$ QW structures, at the wavelength of $1.55 \mu\text{m}$. We have developed IVBA formalisms based on the 6×6 Hamiltonian and applied them to the conventional QW laser structures. We have observed that the absorption increases as barrier decreases

and also that the tensile strain in the structure reduces absorption while compressive strain increases it. We have also observed that higher temperatures reduce the absorption in QWs.

This work is partially supported by Korea Science and Engineering Foundation, OERC-95-02-03-01.

- ¹R. Chin, N. Holonyak, Jr., B. A. Vojak, K. Hess, R. D. Dupuis, and P. D. Dapkus, *Appl. Phys. Lett.* **36**, 19 (1980).
- ²N. K. Dutta and R. J. Nelson, *Appl. Phys. Lett.* **38**, 407 (1981).
- ³T. Uji, K. Iwamoto, and R. Lang, *Appl. Phys. Lett.* **38**, 193 (1981).
- ⁴A. R. Adams, M. Asada, Y. Suematsu, and S. Arai, *Jpn. J. Appl. Phys.* **19**, L621 (1980).
- ⁵M. Asada, A. R. Adams, K. E. Stubkjaer, Y. Suematsu, Y. Itaya, and S. Arai, *IEEE J. Quantum Electron.* **17**, 611 (1981).
- ⁶M. Asada, A. Kameyama, and Y. Suematsu, *IEEE J. Quantum Electron.* **20**, 745 (1984).
- ⁷G. Fuchs, J. Horner, A. Hangleiter, V. Harle, F. Scholz, R. W. Glew, and L. Goldstein, *Appl. Phys. Lett.* **60**, 231 (1992).
- ⁸M. Yano, H. Nishi, and M. Takusagawa, *J. Appl. Phys.* **51**, 4022 (1980).
- ⁹S. Yamakoshi, T. Sanada, O. Wada, I. Umebu, and T. Sakurai, *Appl. Phys. Lett.* **40**, 144 (1982).
- ¹⁰S. Seki, W. W. Lui, and K. Yokoyama, *Appl. Phys. Lett.* **66**, 3093 (1995).
- ¹¹E. P. O'Reilly, *Semicond. Sci. Technol.* **4**, 121 (1989).
- ¹²S. Adachi, in *Properties of Lattice-Matched and Strained Indium Gallium Arsenide*, edited by P. Bhattacharya (INSPEC, London, 1993) Chap. 3, p. 85.
- ¹³S. Adachi, *J. Appl. Phys.* **53**, 8775 (1982).
- ¹⁴T. Cho, H. Kim, S. Hong, and Y. Kwon, *SSDM'95*, 995 (1995).